Science of the Total Environment xxx (xxxx) xxx

Contents lists available at ScienceDirect

Science of the Total Environment

journal homepage: www.elsevier.com/locate/scitotenv

Spatial and seasonal variations of dissolved arsenic in the Yarlung Tsangpo River, southern Tibetan Plateau

Jun-Wen Zhang [a], Ya-Ni Yan [b], Zhi-Qi Zhao [b,*], Xiao-Dong Li [a], Jian-Yang Guo [c], Hu Ding [a], Li-Feng Cui [a], Jun-Lun Meng [c], Cong-Qiang Liu [a,*]

[a] Institute of Surface-Earth System Science, School of Earth System Science, Tianjin University, Tianjin 300072, China
[b] School of Earth Science and Resources, Chang'an University, Xi'an 710054, China
[c] State Key Laboratory of Environmental Geochemistry, Institute of Geochemistry, Chinese Academy of Sciences, Guiyang 550081, China

HIGHLIGHTS

- High levels of dissolved As are observed in YTR system.
- Hot springs are main source of dissolved As in the upper reaches of YTR.
- Natural attenuation of dissolved As in main channel is mainly due to dilution.
- Lowest dissolved As is observed in July and August due to dilution process.
- Weathering of As-containing minerals inputs much of As in rivers in wet-season.

GRAPHICAL ABSTRACT

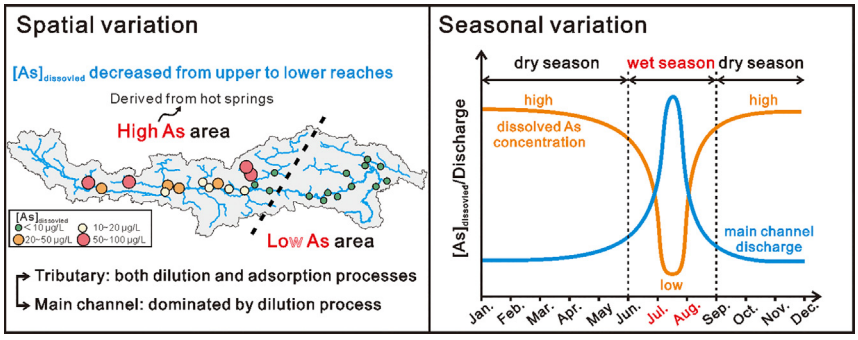

ARTICLE INFO

Article history:
Received 15 August 2020
Received in revised form 10 October 2020
Accepted 28 October 2020
Available online xxxx

Editor: Xinbin Feng

Keywords:
Arsenic
Hydrochemistry
Hot spring
Residence time
Yarlung Tsangpo River

ABSTRACT

High levels of dissolved arsenic (As) have been reported in many rivers running though the Tibetan Plateau (TP), the "Water Tower of Asia". However, the source, spatiotemporal variations, and geochemical behavior of dissolved As in these rivers remain poorly understood. In this study, hot spring, river water, and suspended particulate material samples collected from the Yarlung Tsangpo River (YTR) (upper reaches of the Brahmaputra River) system in 2017 and 2018 were analyzed. Spatial results shown that the upper reaches of YTR (Zone I) have comparatively high levels of dissolved As ($[As]_{dissolved}$: mean 31.7 μg/L; 4.7–81.6 μg/L; n = 16), while the tributaries of the lower reaches (Zone II) have relatively low levels (mean 0.54 μg/L; 0.11–1.3 μg/L; n = 7). Seasonal results shown that the high $[As]_{dissolved}$ (6.1–22.4 μg/L) were found in September to June and low $[As]_{dissolved}$ (1.4–3.7 μg/L) were observed in July to August. Geothermal water is suspected as the main source of the elevated As levels in YTR due to the extremely high $[As]_{dissolved}$ in hot springs (1.13–9.76 mg/L) and abundance of geothermal systems throughout TP. However, the seasonal results suggested that weathering of As-containing rocks and minerals is also a key factor affecting the $[As]_{dissolved}$ in the river water in July to August (wet-season). Natural attenuation of As in main channel is dominated by dilution process due to the lower As concentrations in tributaries, but mostly occurred by both dilution and adsorption (or co-precipitation) processes in tributaries. This work highlights that the weathering process may have an important contribution to the dissolved As in the river waters in wet-season, and the geochemical behavior of As is largely transported conservatively in the main channel and relative non-conservatively in the tributaries in YTR system.

* Corresponding authors.
E-mail addresses: zhaozhiqi@chd.edu.cn (Z.-Q. Zhao), liucongqiang@tju.edu.cn (C.-Q. Liu).

https://doi.org/10.1016/j.scitotenv.2020.143416
0048-9697/

1. Introduction

As the "Water Tower of Asia", the Tibetan Plateau (TP) is the source of many large rivers in Asia, including the Yarlung Tsangpo River (YTR) (upper reaches of the Brahmaputra River), Indus River, Ganges River, Salween River, Mekong River, Yangtze River, and Yellow River. These rivers sustain life and are sources of agricultural and industrial water supplies for about 40% of the world's population, including China and India (Xu et al., 2008). The upper reaches of these rivers are generally considered to be free from contamination due to their relatively pristine environment (Huang et al., 2008). However, since the increase in anthropogenic activities (e.g., agricultural and industrial activities, and urbanization) in TP, some rivers have been contaminated by heavy metals, such as arsenic (As), cadmium (Cd), and lead (Pb) (Qu et al., 2019 and the references therein). Recently, C. Yu et al. (2019) suggested that climate warming-enhanced thawing of permafrost may accelerate release and mobilization of trace elements (e.g., As) into the rivers of TP. Seasonal variations in precipitation and surface run-off strongly affect river discharge, which in turn affects the concentration of heavy metals in river water. Although few people live in TP, rivers originating in TP have a direct (or indirect) effect on water quality of surface water and groundwater utilized by the densely populated regions located downstream. Therefore, there is an urgent need to investigate the spatial and temporal variations of river water chemistry in TP.

High levels of As have been observed in some head waters of rivers in TP, such as the Singe Tsangpo (252 μg/L, upper reaches of the Indus River), Mayum Tsangpo (262 μg/L, head waters of YTR), Naqu (38.9 μg/L, head waters of the Salween River), Tuotuo River (52.2 μg/L, head waters of the Yangtze River), and the upper reaches of the Yellow River (77.1 μg/L) (Guo et al., 2008; Huang et al., 2011; Li et al., 2013; C. Li et al., 2014; Tian et al., 2016; C. Yu et al., 2019), which far exceed the recommended level of 10 μg/L in drinking water proposed by the World Health Organization (WHO), as well as the mean value 0.62 μg/L of the world's rivers (Gaillardet et al., 2003; WHO, 2011). Similarly, enrichment of As has also been reported in rivers in other regions of the world, such as the northern Rocky Mountains of western Montana (USA) (10–370 μg/L) and the Altiplano-Puna plateau of Argentina, Bolivia, Chile, and Perú (8.6–13,000 μg/L) (Nimick et al., 1998; Romero et al., 2003; Concha et al., 2010; Muñoz et al., 2015; Tapia et al., 2019). Notably, many of As-enriched rivers (including those in TP) and high As groundwater are distributed in (or close to) major orogenic belts, which are characterized by an abundance of geothermal systems (Nordstrom et al., 2005, Nordstrom, 2009; Guillot and Charlet, 2007; Mukherjee et al., 2014).

YTR is the largest river system draining the Himalayan Mountain and southern TP, and transports a significant portion of weathered materials to downstream (Hren et al., 2007). Hence, high As concentration in YTR system continues to attract more and more attention (Wang et al., 2012; Li et al., 2013; C. Li et al., 2014; Guo et al., 2015; Tian et al., 2016; Qu et al., 2019). Significantly elevated As concentrations have been reported in many of the tributaries of YTR, such as the Mayum Tsangpo (262 μg/L), Dargye Tsangpo (72 μg/L), Dogxung Tsangbo (50 μg/L), and Duilong Qu (206 μg/L) (Huang et al., 2011; C. Li et al., 2014; Y. Zhang et al., 2015). Weathering of As-enriched rock and minerals, mining activities, salinity of lakes and As-riched hot springs are considered as potential sources of As in these rivers (Li et al., 2013; Y. Zhang et al., 2015; Guo et al., 2015). In TP, As-riched rivers are mainly found in the upper reaches of YTR, while the downstream usually contain relatively low levels of As. Moreover, river water in the downstream (the Brahmaputra River) usually contain relatively low As concentrations of less than 3 μg/L (Islam et al., 2012).

Adsorption of dissolved As by river sediments and dilution process are considered to be the main causes for natural attenuation of dissolved As in Zangbu Qu near the Yangbajain geothermal field (Guo et al., 2015). However, Nimick et al. (1998) suggested that geothermal dissolved As is transported largely conservative in the larger Madison River system and the decrease in As concentration along the river is almost exclusively caused by dilution. The dissolved As concentration in river water is also affected by the seasonal variation in precipitation, river temperature, and melt water, however, there few studies on the seasonal variation in As concentration in YTR (e.g., Masson et al., 2007; Zhao et al., 2020). Although the As concentration in YTR tends to decrease from upstream to downstream, significantly greater concentrations of As have been widely reported in groundwater of the downstream floodplains, such as India and Bangladesh (e.g., Nickson et al., 1998, 2000; Nordstrom, 2002; Smedley and Kinniburgh, 2002; Fendorf et al., 2010; Wang et al., 2017; Mukherjee, 2018). At present, the source, temporal and spatial variations, and geochemical behavior of As throughout YTR system remain poorly understood.

In this study, dissolved As in the river water (including monthly water samples in a year), suspended particulate material (SPM) and hot spring samples collected from YTR system were evaluated in order

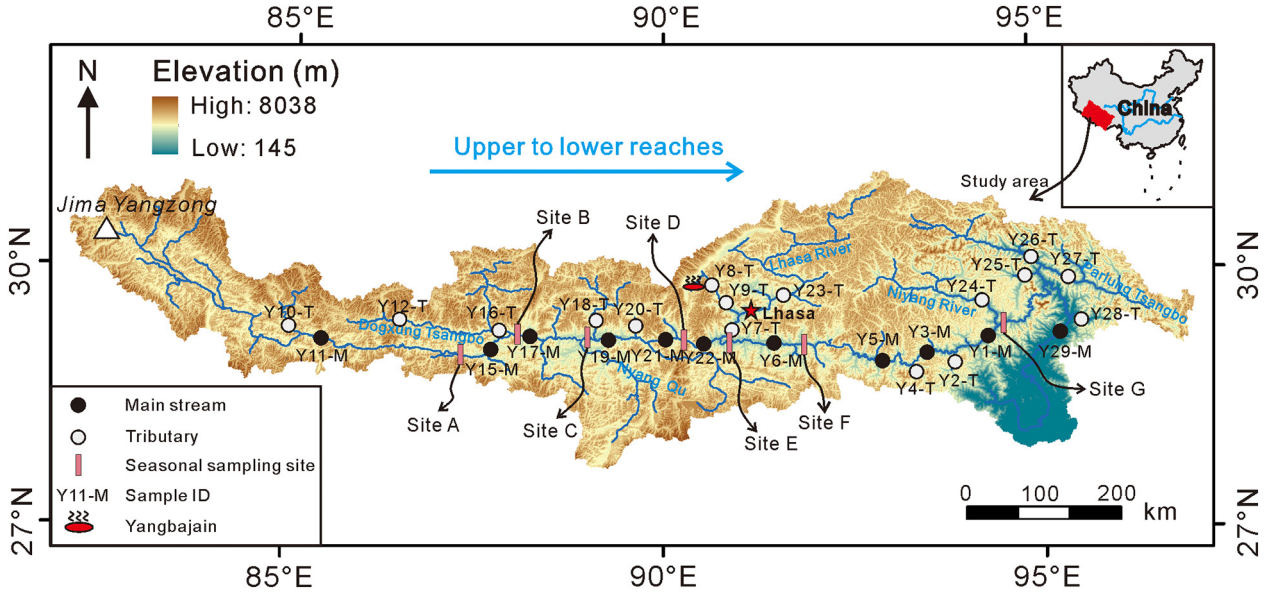

Fig. 1. Sampling sites in YTR system, southern TP.

to: 1) identify the source and distribution of dissolved As in YTR, 2) elucidate the mechanism underlying the temporal and spatial variations of dissolved As along YTR, and 3) assess the geochemical behavior of As in river water in YTR basin.

2. Study area

YTR is the largest river system of TP, originated from *Jima Yangzong* glacier at Mount Kailash in the northern Himalayas (Fig. 1) (Huang et al., 2008). It flows eastward for about 1300 km along the Indus-Tsangpo suture between the Indian and Eurasian tectonic plates (Hren et al., 2007), then it flows southwest with a sharp drop in elevation near Namche Barwa and subsequently into India. In India, YTR is known as the Brahmaputra River and then it joins the Ganges River, passing through Bangladesh, and finally flows into the Bay of Bengal. The catchment area and mean annual discharge of YTR basin are ~24×10^4 km^2 and ~1395.4×10^8 m^3, respectively (Liu et al., 2007). Mean annual precipitation along YTR is about 495 mm, which decreases from 5000 mm in the low reaches to 200 mm near the head waters, and the mean annual air temperature is about 5.9 °C (Huang et al., 2011, and the references therein). More than 80% of the annual precipitation is concentrated in the period of June to September, with the exception of parts of southeastern Tibet (Fig. 2(a)). In the present study, July and August are defined as the wet-season. Mean annual evaporation is 1052 mm in this area (You et al., 2007). The river water is mostly recharged by glacier/snow melt water and groundwater (e.g., springs) in the head waters and upper reaches of the basin, and mainly by precipitation, as well as some melt water and groundwater, in the middle and lower reaches (Liu, 1999). YTR has a large number of tributaries, most of which originated from glaciers, including the Dogxung Tsangbo, Nyang Qu, Lhasa River, Niyang River, and Parlung Tsangbo, both having a catchment area larger than 1×10^4 km^2 (Liu, 1999) (Fig. 1). Due to the influx of the tributaries, the main channel discharge of YTR is several folds greater downstream than that of upstream. According to Liu et al. (2007), the mean annual discharge of main channel from 1956 to 2000 in the Lhatse hydrological station (adjacent to Lhatse county) was ~56.2×10^8 m^3, which was significantly increased to ~605.7×10^8 m^3 in the Nuxia hydrological station (adjacent to Nyingchi city). The annual discharge of main channel is mainly concentrated from June to October, reaching the maximum in August (Fig. 2(b)).

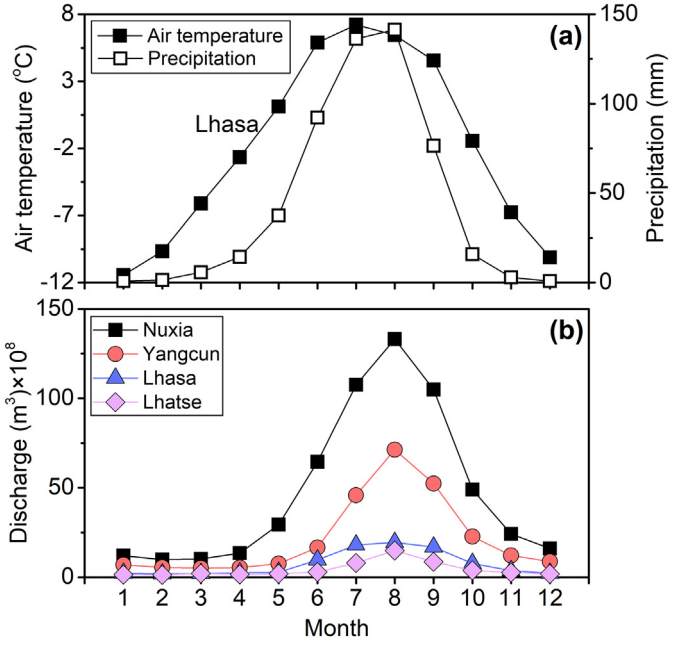

Fig. 2. Monthly air temperature and precipitation of Lhasa, and river discharge in hydrological station of Nuxia, Yangcun, Lhasa, and Lhatse in YTR basin. The location of the hydrological stations is present in Fig. S1. Data of air temperature and precipitation in Lhasa are from F. Li et al. (2014). Data of discharge in hydrological stations are from Gao et al. (2007).

Geologically, YTR basin is developed along the collisional suture zone of the Indian and Eurasian tectonic plates (Aitchison et al., 2002). This narrow basin extends from west to east and turns northeast to southwest near Namche Barwa in the eastern syntaxis of the Himalayas. The southern part of the basin is located in the Himalayan Mountains, while the north part is located in the Gangdise Mountains and Nyenchen Tanglha Mountains. Generally, the terranes of the southern TP are dominated by Palaeozoic-Mesozoic carbonate and clastic sedimentary rocks, such as conglomerate and sandstone (Hren et al., 2007). In parts of the northeastern and northwestern areas, it is dominated by Cretaceous-Tertiary granitic plutons, consisting of gabbroic to granodioritic rock, and Tertiary volcanics, respectively. The eastern Himalayan syntaxis is a highly metamorphic zone that mainly consists of migmatitic gneisses and metamorphism granulite facies. Additionally, rock outcrops of ophiolites and ophiolitic melanges are commonly found along the entire course of YTR (Huang et al., 2011).

3. Materials and methods

3.1. Sampling and field measurement

A total of 123 river water and SPM samples were collected in YTR system (Fig. 1). Spatial variations of river water and SPM samples were collected from YTR basin in June 2017, including, 11 samples from the main channel and 16 samples from the tributaries, respectively. The tributaries with relatively large catchment area were mainly selected for sampling. The main channel sampling sites were mainly set before or after the inflow of the large tributaries, and were roughly evenly distributed throughout YTR basin. Seasonal variations of river water samples were collected monthly from October 2017 to September 2018, with the exception of November 2017, and 77 river water samples were obtained from seven fixed sampling sites (site A to site G) distributed in the upper reaches to lower reaches in main channel. The main channel was usually dispersed into multiple channels in the upper reaches. Thus, sampling was usually carried out on the riverside where these channels were merged into one to ensure the representativeness of the collected samples. Moreover, the main channel sampling sites are at least 1 km downstream from the inflow of the tributaries to ensure that the water from tributaries and main channel are fully mixed and homogeneous. The SPM was filtered from the water samples. Some SPM from the tributaries were not sampled because the river water was clear and had little SPM. In addition, a hot spring sample was collected from the Yangbajain geothermal field, central TP. The temperature (T), pH, dissolved oxygen (DO) and electrical conductivity (EC) of each water sample were measured in situ using a portable multi-parameter meter after calibration. The pH electrode was calibrated using buffers with pH 4.01, 7.00, and 10.01. Alkalinity was measured using the Gran titration method within 24 h. Each water sample was filtered through a 0.45 μm cellulose membrane immediately in the field. Then, for the analysis of major cations and trace elements, water samples were stored in acid washed 120 mL high-density polyethylene bottles and acidified with double-distilled HNO_3 to pH < 2. For anions, water samples were stored in pre-cleaned 15 mL centrifuge tubes without acidification. SPM was collected on the filter membranes and rinsed into pre-cleaned 50 mL centrifuge tubes using ultra-pure water. All of the samples were stored at 4 °C until laboratory analysis.

3.2. Laboratory analysis

Major cations and anions concentrations in water samples were analyzed by inductively coupled plasma optical emission spectrometry (ICP-OES) and ion chromatography, respectively. After drying, each

SPM sample was homogenized and then ground in an agate mill and passed through a 200 mesh nylon sieve. After acid digestion, major elements (e.g., Al, and Fe) and trace elements (e.g., As) in SPM were determined by ICP-OES and ICP mass spectrometry, respectively. At the same time, laboratory standard solutions and blanks were determined to ensure the data quality. The precision for most major ions (cations and anions) and trace elements is better than ±5% (2σ) and ±10% (2σ), respectively. All analyses were conducted at the State Key Laboratory of Environmental Geochemistry, Institute of Geochemistry, Chinese Academy of Sciences.

4. Results

4.1. Dissolved As in hot springs

The pH of the geothermal water samples was neutral to weakly alkaline (mean 8.1; 7.30–8.85) (Table 1). Although Eh value of the samples was not measured this time, it varies from −300 to 0 mv in most geothermal water of TP (Liu, 2018; Liu et al., 2019). Total dissolved concentration of As ($[As]_{dissolved}$) in the Yangbajain hot spring sample was 3.72 mg/L, which fell within the range of the reported $[As]_{dissolved}$ in hot springs of the Yangbajain geothermal field (mean 3.22 mg/L; 2.70–3.84 mg/L; n = 19) (Guo, 2012; Li et al., 2013; Liu, 2018). The hot spring was also enriched with part of major elements (Na: 378 mg/L, Cl: 432 mg/L) and trace elements (Li: 9.50 mg/L, B: 49.4 mg/L, Cs: 4.02 mg/L). These values were consistent with the published data from other geothermal fields in TP (Fig. S1), including the Dagejia, Semi and Yangyi (Table 1) (e.g., Guo, 2012; Yuan et al., 2014; Y. Zhang et al., 2015; Liu, 2018). According to Guo et al. (2019), these high As (>1.5 mg/L) geothermal waters are chloride-type, with the exception of the Yangyi.

4.2. Spatial variations of dissolved As in river waters

Chemical compositions of river water samples are presented in Table 1. The study area was divided into Zone I and Zone II based on the variation of chemical composition in river water samples. The concentrations of As, B, Cs, and Li and the ratios of As/Cl, B/Cl, and Cs/Cl in river water had distinct inflection points between the samples Y5-M and Y6-M along the main channel (Fig. 4). The $[As]_{dissolved}$ in river waters varied from 0.11 to 81.6 μg/L. Notably, $[As]_{dissolved}$ in 13 (48.1%) of the 27 river water samples from the upper reaches of YTR basin (Zone I) exceeded the guideline of 10 μg/L in drinking water recommended by WHO (Fig. 3(a)). In contrast, $[As]_{dissolved}$ in river waters from the lower reaches of the river basin (Zone II) was less than 10 μg/L. Additionally, $[As]_{dissolved}$ in tributaries of Zone I was relatively high (mean 41.2 μg/L; 4.7–81.6 μg/L), while the content of most samples from Zone II was less than 1 μg/L. The $[B]_{dissolved}$, $[Cs]_{dissolved}$, and $[Li]_{dissolved}$ in most of river water samples were significantly higher than the mean values of the world's rivers (Table 1) (Gaillardet et al., 2003). Interestingly, the distribution of $[B]_{dissolved}$, $[Cs]_{dissolved}$, $[Li]_{dissolved}$, $[Na]_{dissolved}$, and $[Cl]_{dissolved}$ in river waters were similar to that of $[As]_{dissolved}$ (Fig. S2). That is, these elements are enriched in Zone I, while the concentrations in Zone II are relatively low.

Variations in $[As]_{dissolved}$, $[B]_{dissolved}$, $[Cs]_{dissolved}$, $[Li]_{dissolved}$, $[Na]_{dissolved}$, and EC, as well as the molar ratios of these elements to Cl along the flow direction are presented in Fig. 4. In main channel, $[As]_{dissolved}$, $[B]_{dissolved}$, $[Cs]_{dissolved}$, $[Li]_{dissolved}$, $[Na]_{dissolved}$, and EC gradually decreased along the river flow direction. The $[As]_{dissolved}$, $[B]_{dissolved}$ and $[Cs]_{dissolved}$ in river water samples had similar trends along the main channel, which had significantly decreased from 0 to 900 km (Zone I) and then decreased slowly afterward (from sample Y5-M). Similarly, molar ratios of As/Cl, Cs/Cl, and B/Cl in river water samples sharply decreased from 0 to 900 km and keeping relatively stable between 900 and 1600 km. In contrast, Na/Cl ratio kept relatively stable along throughout the river flow (2.32–2.86) (Table 1). As to the tributaries, $[As]_{dissolved}$, $[B]_{dissolved}$, $[Cs]_{dissolved}$, $[Li]_{dissolved}$, $[Na]_{dissolved}$, and EC in river waters showed a trend of decrease from the upper reaches (Zone I) to the lower reaches (Zone II) of studied catchment. In general, the relatively low concentrations of these elements were observed in tributaries of Zone II. Similarly, the ratios of As/Cl, B/Cl, and Cs/Cl showed a decreasing tendency from the upper to the lower reaches. In contrast, the Na/Cl ratio kept relatively stable (1.86–4.55) in tributaries of Zone I, but was significantly increased in tributaries of Zone II (5.80–34.45) (Table 1).

4.3. Seasonal variations of dissolved As in river waters

Seasonal variations of $[As]_{dissolved}$, As/Cl, Na/Cl, and EC values in river waters from the seven fixed sampling sites are present in Fig. 5. The higher (6.1–22.4 μg/L) and lower (1.4–3.7 μg/L) values of $[As]_{dissolved}$ in river waters were observed in September to June and July to August during the sampling time period, respectively, with the exception of the site G. Most of As/Cl value decreased gradually from October to February and showed an increasing tendency afterwards. The Na/Cl value kept relatively constant from October to June and increased significantly in July and August, and then decreased sharply afterwards. Most of EC value kept relatively stable during the sampling period, but declined significantly in July and August. However, in July and August, the $[As]_{dissolved}$ kept relatively constant while the As/Cl value showed an increasing trend in river waters from site A to site G.

4.4. Relationship between Cl and As, B, Cs, Li, Na in hot springs and river waters

$[As]_{dissolved}$, $[B]_{dissolved}$, $[Cs]_{dissolved}$, $[Li]_{dissolved}$ and $[Na]_{dissolved}$ were positively correlated with $[Cl]_{dissolved}$ in hot springs and river waters (Fig. 6). The X vs. Cl (X refers to As, B, Cs, or Li) data points tend to be lower than the theoretical dilution line of hot springs, especially for As and Cs, while all of the data points of a graph of Na vs. Cl were within the range of the theoretical dilution line of hot springs, with the exception of the tributaries of Zone II. It was worth noting that the main channel data points of As vs. Cl, B vs. Cl, and Cs vs. Cl showed two different trends (trend 1 and trend 2) in Zone I and Zone II. The trend 1 was at an angle to the dilution and was biased in the counterclockwise direction of the dilution line. However, the trend 2 was almost parallel to the dilution line.

4.5. Content of As in SPM

SPM concentrations in river water samples varied between 0.76 and 409 mg/L. In main channel, SPM concentrations ranged from 2.3 to 11.5 mg/L (mean 5.7 mg/L), except that the sample of Y29-M (408.8 mg/L). Contents of Al, Fe, and Mn in SPM ranged from 8.31% to 11.44%, 2.79% to 12.38%, and 0.04% to 0.76%, respectively. Arsenic contents in SPM samples were extremely high (mean 117 mg/kg; 36.6–615 mg/kg). These values were much higher than those of unconsolidated sediments (3–10 mg/kg, Smedley and Kinniburgh, 2013), and the upper continental crust (mean 5.7 mg/kg, Hu and Gao, 2008). Moreover, there was a strong positive correlation ($R^2 = 0.97$, $p < 0.01$) between As and Mn contents in SPM samples (Fig. S3).

5. Discussion

5.1. Enrichment of As in YTR

High levels of $[As]_{dissolved}$ are observed in river waters of the Yarlung Tsangpo basin, with the exception of the tributaries in Zone II (Fig. 3). This observation is consistent with the results from previous studies in the basin (e.g., Li et al., 2013; Y. Zhang et al., 2015; Guo et al., 2015). Generally, As is enriched in hot springs and has been observed in geothermal systems of TP (e.g., Yuan et al., 2014; Y.F. Zhang et al., 2015; Liu

Table 1
Physical parameters and chemical components in river waters and hot springs from YTR.

Sample ID	Longitude	Latitude	Elevation m	T °C	DO mg/L	EC μS/cm	pH	Ca^{2+} mg/L	K^+ mg/L	Mg^{2+} mg/L	Na^+ mg/L	Cl^- mg/L	HCO_3^- mg/L	SO_4^{2-} mg/L	Li μg/L	B μg/L	As μg/L	Cs μg/L	Na/Cl mol/mol	Li/Cl mol/mol×1000	B/Cl mol/mol	As/Cl mol/mol×1000	Cs/Cl mol/mol×1000
Upper reaches (Zone I)																							
Y11-M	29°19′17″	85°10′07″	4457	11.8	6.0	363.0	8.25	42.0	1.7	6.9	19.2	10.4	130.5	57.7	143.8	3497	46.6	67.5	2.86	70.4	1.09	2.13	1.74
Y15-M	29°10′51″	87°40′29″	3951	15.8	6.4	352.0	8.56	44.7	1.9	8.6	13.9	9.3	145.2	42.8	128.1	2052	17.6	65.8	2.32	70.1	0.71	0.90	1.90
Y17-M	29°21′56″	88°07′27″	3874	16.0	6.3	324.0	8.62	39.3	1.8	7.4	14.8	9.1	123.2	39.4	112.6	1766	20.6	48.4	2.51	62.8	0.63	1.07	1.42
Y19-M	29°20′13″	89°11′20″	3812	15.2	6.0	303.0	8.61	36.6	1.7	6.9	13.9	7.7	120.2	35.2	102.4	1464	15.9	35.2	2.78	67.5	0.61	0.98	1.22
Y21-M	29°19′15″	89°55′57″	3702	17.5	6.4	307.0	8.65	36.2	1.7	7.2	14.8	9.6	109.2	38.3	122.6	1501	14.9	35.9	2.37	64.6	0.50	0.73	1.00
Y22-M	29°19′35″	90°40′20″	3594	19.4	6.7	300.0	8.64	35.6	1.7	7.1	14.4	8.8	119.0	37.3	106.5	1433	13.8	31.8	2.54	61.6	0.53	0.75	0.97
Y6-M	29°16′23″	91°32′13″	3555	17.4	6.6	281.0	8.50	33.9	1.6	6.8	11.3	7.0	109.2	38.4	85.7	812	7.6	8.7	2.48	62.0	0.37	0.51	0.33
Y10-T	29°19′46″	85°09′14″	4477	11.9	5.8	377.0	8.28	43.0	1.7	6.8	21.6	11.1	131.2	65.2	173.8	4009	56.0	83.5	3.01	79.6	1.17	2.39	2.01
Y12-T	29°30′26″	86°27′46″	4626	13.3	6.5	322.0	8.63	36.3	1.7	5.6	19.6	7.2	107.4	60.2	130.3	3070	76.6	31.2	4.21	91.9	1.38	5.04	1.16
Y16-T	29°23′51″	87°57′16″	3950	17.3	6.9	264.0	8.67	28.0	1.8	4.8	17.5	9.2	95.8	35.0	90.6	1223	31.9	23.3	2.94	49.8	0.43	1.64	0.67
Y18-T	29°27′09″	89°05′48″	3865	10.8	5.8	259.0	8.27	26.9	1.7	5.1	16.4	5.6	101.3	31.5	76.8	827	11.8	17.5	4.49	69.2	0.47	0.99	0.83
Y20-T	29°21′50″	89°38′04″	3756	12.5	6.8	293.0	8.48	34.3	1.5	5.2	14.1	4.8	79.9	67.6	63.3	1486	32.0	6.4	4.55	67.0	1.00	3.17	0.36
Y8-T	30°03′09″	90°35′31″	4140	13.0	6.5	158.8	8.52	12.1	2.5	0.9	16.5	13.5	51.9	8.7	309.2	1636	81.6	91.3	1.89	116.3	0.39	2.86	1.81
Y9-T	29°42′27″	90°52′25″	3829	17.9	6.2	197.9	8.33	17.6	2.7	1.5	17.8	14.7	65.3	14.6	313.2	1764	68.4	82.1	1.86	107.7	0.39	2.20	1.49
Y7-T	29°28′47″	90°56′08″	3615	16.2	6.8	249.0	8.47	30.6	1.4	6.3	8.6	5.6	51.9	32.7	75.0	375.2	7.3	11.5	2.38	68.4	0.22	0.62	0.55
Y23-T	29°48′20″	91°34′45″	3756	13.7	6.8	207.0	8.48	26.4	1.1	5.5	5.7	3.5	31.1	32.4	44.4	219	4.7	8.4	2.53	64.6	0.20	0.64	0.64
Lower reaches (Zone II)																							
Y5-M	29°04′00″	92°55′44″	3059	19.7	6.8	274.0	8.77	32.9	1.7	6.8	12.4	7.6	104.3	38.1	94.6	1018	9.5	8.5	2.51	63.0	0.43	0.59	0.30
Y3-M	29°06′25″	93°27′06″	2985	16.9	7.1	270.0	8.55	32.1	1.5	6.5	10.8	6.8	98.8	39.3	77.5	881	7.3	7.9	2.43	57.6	0.42	0.51	0.31
Y1-M	29°16′39″	94°18′46″	2915	14.8	7.6	164.7	8.34	19.8	0.9	3.8	5.6	3.4	60.4	23.9	40.5	455	3.9	3.8	2.56	60.4	0.43	0.54	0.30
Y29-M	29°26′26″	95°24′30″	709	16.8	10.0	123.4	8.17	17.2	1.0	2.9	1.9	1.1	51.2	17.6	10.6	80.7	1.3	0.57	2.61	46.9	0.23	0.53	0.13
Y4-T	28°59′56″	93°19′16″	3003	11.8	7.5	230.0	7.81	26.9	0.3	8.8	1.9	0.17	32.9	81.9	8.6	14.3	0.11	0.36	16.92	257.9	0.27	0.31	0.57
Y2-T	29°07′18″	93°52′05″	2943	8.7		62.0	7.80	8.7	0.3	1.4	0.78	0.18	22.0	10.0	0.88	2.1	0.56	0.01	6.58	24.4	0.04	1.46	0.01
Y24-T	29°30′56″	94°25′48″	2913	12.7	7.4	82.0	7.80	11.5	0.6	2.1	1.7	0.45	31.1	12.3	2.7	33.2	0.64	0.75	5.80	30.6	0.24	0.67	0.44
Y25-T	29°59′37″	94°52′50″	2362	14.1	7.2	95.3	8.07	14.5	1.5	1.3	1.0	0.05	40.9	10.8	0.53	3.3	0.20	0.02	34.35	58.9	0.23	2.05	0.14
Y26-T	30°05′50″	95°03′58″	2018	11.2	8.9	125.5	8.22	7.8	0.4	1.6	0.84	0.10	22.6	8.6	1.7	4.1	0.51	0.08	12.86	87.5	0.13	2.39	0.22
Y27-T	29°54′26″	95°28′44″	2603	10.9	8.4	122.2	8.46	17.9	1.0	3.6	1.0	0.13	56.7	13.6	2.0	14.0	1.3	0.09	12.35	77.7	0.35	4.93	0.18
Y28-T	29°42′37″	95°35′09″	2746	8.2	8.4	63.2	8.54	10.9	0.5	1.1	0.53	0.05	30.5	7.0	0.48	1.6	0.48	0.03	18.04	54.0	0.11	5.00	0.20
World's rivers Mean															1.84	10.2	0.62	0.011					

Hot spring	Longitude	Latitude	Elevation m	EC μS/cm	pH	Ca^{2+} mg/L	K^+ mg/L	Mg^{2+} mg/L	Na^+ mg/L	Cl^- mg/L	Li mg/L	B mg/L	As mg/L	Cs mg/L	Na/Cl mol/mol	Li/Cl mol/mol	B/Cl mol/mol	As/Cl mol/mol	Cs/Cl mol/mol
Yangbajain[a]	30°04′48″	90°28′56″	4289	2100	8.85				378	432	9.50	49.4	3.72	4.02	1.35	0.11	0.37	0.004	0.002
Dagejia[b]				1867	8.36	21.3	51.0	0.67	432	152	5.25	99.5	8.92	5.97	4.39	0.18	2.11	0.028	0.010
Semi[b]				3440	7.34	165.1	107.0	9.1	599	501	18.0	343.4	9.76	31.7	1.85	0.18	2.21	0.009	0.017
Xietongmen[b]					7.30	109.7	55.3	7.7	550	816	17.7	275.4		12.1	1.04	0.11	1.09		0.004
Yangyi[b]				1074	8.09	41.3	23.4	8.4	279	97	5.69	21.3	1.13	0.55	4.44	0.30	0.71	0.006	0.002
Yangbajain[b]				2299	8.76	24.7	59.2	0.78	376	491	8.44	50.7	3.22	4.98	1.18	0.09	0.33	0.003	0.003

[a] Analyzed in this study.
[b] Mean values of published data from Dagejia (n = 15), Semi (n = 7), Xietongmen (n = 1), Yangyi (n = 4), Yangbajain (n = 18) geothermal fields (Li, 2002; Guo et al., 2008; Guo, 2012; Li et al., 2013; Liu, 2018). The world's rivers mean value of trace elements from Gaillardet et al. (2003).

et al., 2019). Coupled with the abundance of geothermal systems in TP (Kearey and Wei, 1993; Guo, 2012), hot springs could be an important source of As in rivers of TP (e.g., C. Li et al., 2014). Chlorine is a relatively conservative element that is also enriched in hot springs of the study area. Thus, the main evidence for this view is the good positive correlation between As and Cl in all river samples ($R^2 = 0.57$, $p < 0.01$) (Fig. S4), and the data points of river water distributed near the theoretical (or conservative) dilution lines of the hot springs (Fig. 6(a)). The $[B]_{dissolved}$, $[Cs]_{dissolved}$, and $[Li]_{dissolved}$ in most of river water samples are significantly higher than the mean values of the world's rivers (Table 1) (Gaillardet et al., 2003). Also, since the B, Cs, and Li are enriched in hot springs in TP, there is a similar relationship between $[Cl]_{dissolved}$ and $[B]_{dissolved}$, $[Cs]_{dissolved}$, and $[Li]_{dissolved}$ (Fig. 6). These results further confirm that hot springs are the source of the elevated As levels in YTR. This finding is consistent with the results of previous studies in the Madison River that the river water is enriched in As, B, and Li due to input of hot springs from Yellowstone National Park, which is mostly located in the state of Wyoming and parts of the states of Montana and Idaho, USA (Nimick et al., 1998; Ball et al., 2010). Similar results have also been reported in Rio Loa River (Chile) and Sarouq River (Iran), which is located near geothermal fields (Romero et al., 2003; Sharifi et al., 2016).

Certainly, there are other reasons that may also lead to the enrichment of As in river water. Salt lakes and evaporite may be important sources of As in the study area (Li et al., 2013). However, because the major chemical compositions of salt lakes are similar to those of hot springs in this area (Yu et al., 2013), it is difficult to distinguish and quantify their contributions to the elevated As concentrations in river water in this study. On the other hand, previous studies have reported that geothermal water is the primary source of some trace elements (e.g., As, B, Cs, and Li) in salt lakes of TP (e.g., Zheng and Liu, 2009).

5.2. Spatial variations of dissolved As in river waters

Although the input of hot springs led to the enrichment of As in the upper reaches, $[As]_{dissolved}$ in river waters is reduced downstream by several ten-fold. As shown in Fig. 4, $[As]_{dissolved}$ ($[B]_{dissolved}$, $[Cs]_{dissolved}$, and $[Li]_{dissolved}$) in main channel of YTR gradually decreased further downstream. Similar results were observed in other rivers contaminated by hot springs. Dilution and adsorption processes are considered to be the main mechanisms underlying the natural attenuation of these elements in rivers (Nimick et al., 1998; Guo et al., 2015). Moreover, As, B, and Li are thought to be transported conservatively in the Madison River, as confirmed by the concentrations of these elements fall along the theoretical dilution lines of hot springs. In contrast, some concentration for these elements do not fall within the theoretical dilution line ranges of hot springs in the present study, especially for As and Cs (Fig. 6). In addition, there are two distinctly different trends of the data points from the high concentration to low concentration. The trend 1 may reflect removal of partial dissolved As from river water, while the trend 2 reflects the dilution process due to its almost parallel to the theoretical dilution line (Nimick et al., 1998). Thus, we concluded that the decrease in $[As]_{dissolved}$ in main channel of YTR is primarily due to dilution, while in tributaries in Zone I, this decrease is due to both the dilution and adsorption processes, as discussed below.

5.2.1. Effect of dilution in main channel of YTR

Dilution is the main mechanism underlying the natural attenuation of As in main channel, as supported by the significant decrease in $[As]_{dissolved}$ in the incoming tributaries from the upper to lower reaches of YTR basin (Fig. 4(a)). In addition, the decrease in EC value along the main channel indicates that river water is diluted by melt waters (e.g., glaciers) (Fig. 4(k)), which have low levels of As (Li et al., 2013). On the other hand, as there is little precipitation in the upper reaches of the catchment, the river water quality will reflect the underlying groundwater (e.g., hot springs). However, as precipitation increased in the lower reaches, the effect of dilution becomes significant in this area. Certainly, this mechanism cannot rule out the effects of adsorption process in the natural attenuation of As, and needs further discussion.

Generally, element Cl is considered to be conserved in hydrologic cycle (e.g., Roy et al., 1999). Accordingly, variation in the ratio of an element to Cl can be used to determine if the element has been lost from the river (decreased ratio), is stable (relatively constant ratio), or has been added (increased ratio). For example, $[Na]_{dissolved}$ tend to decrease with increasing flow distance in main channel, although the Na/Cl ratio keeps mostly constant (Fig. 4). Therefore, dilution is the main cause of the decrease in $[Na]_{dissolved}$ in main channel. In contrast, $[As]_{dissolved}$ and As/Cl ratio in main channel decrease with increasing flow distance. Similar variations of $[B]_{dissolved}$, $[Cs]_{dissolved}$, and $[Li]_{dissolved}$, and B/Cl, Cs/Cl, and Li/Cl ratios are observed in main channel. Superficially, this observation can be attributed to the loss of As, B, Cs, and Li in main channel river waters via the adsorption process (or other processes). However, compared with the relatively constant Na/Cl ratio in tributaries (Zone I), the As/Cl ratio greatly varied and tend to decrease from upper to lower reaches of the basin, which is similar to the variations of $[As]_{dissolved}$ in tributaries (Fig. 4). Thus, the influx into the tributaries with relatively low As/Cl ratios will necessarily decrease the As/Cl ratio in main channel. Although some tributaries in Zone II have relatively high As/Cl and Na/Cl ratios, these tributaries do not significantly affect the As/Cl and Na/Cl ratios of main channel in this region because of very low $[As]_{dissolved}$ and flux as compared with the main channel. So these tributaries contribute very little to the total content of As (and Cl) in main channel, as confirmed by the relatively constant As/Cl ratio in main channel of Zone II (Fig. 4(b)). Accordingly, the decrease in As/Cl ratios along the main channel is partly caused by the influx of with relatively lower As/Cl ratios in tributaries.

The limited contribution of adsorption to natural attenuation of As in main channel is also supported by the low concentration of SPM in river water. The low SPM concentration in main channel is mainly due to the gradual decrease in elevation and relatively slow water flow, with the exception of sample Y29-M (Fig. 4(m)). In contrast, the SPM concentration is relatively high in sample Y29-M (408.8 mg/L) because of the accelerated flow of rushing water that is mainly caused by the sharp drop in elevation (from about 3000 to 709 m). The strong adsorption capacity for As of SPM is due to high contents of Fe, Al, and Mn oxides or hydroxides (or clay minerals) (Table S1). However, based on As concentrations in the filtered water and SPM, the calculated results (except for sample Y29-M) suggest that the content of As in the SPM is generally less than 5% of total content As in river water (sum of suspended and dissolved loads), suggesting that the SPM removes very little As from river water. On the other hand, there may be insufficient available sorption sites (saturated) in SPM, which has been exposed to high As concentrations in tributaries (upper reaches) (Nimick et al., 1998), suggesting that As is largely conserved in main channel. In other words, the dilution process plays a major role in reducing the $[As]_{dissolved}$ in main channel of YTR.

5.2.2. Effect of dilution and adsorption in tributaries of Zone I

As mentioned in Section 5.2.1, dilution is the main mechanism of natural attenuation of As in main channel. Similarly, the flow of water from hot springs into the tributaries is also significantly affected by dilution, resulting in decreased $[As]_{dissolved}$ in tributaries by several fold that of hot springs. Assuming that dilution is the only mechanism of the natural attenuation of As in the studied catchment, then all of the concentration data points (As vs. Cl) of tributaries and main channel should be within the range of the theoretical dilution line of hot springs (Fig. 6). However, in fact, most of these data points tend to deviate downward from the theoretical dilution line, indicating that some of $[As]_{dissolved}$ is lost from river water. Therefore, there must be other factors affecting the geochemical behavior of As in these tributaries.

Significantly decrease in $[As]_{dissolved}$ and As/Na ratio in river waters is observed in the Dogxung Tsangbo, indicating that part of dissolved As is

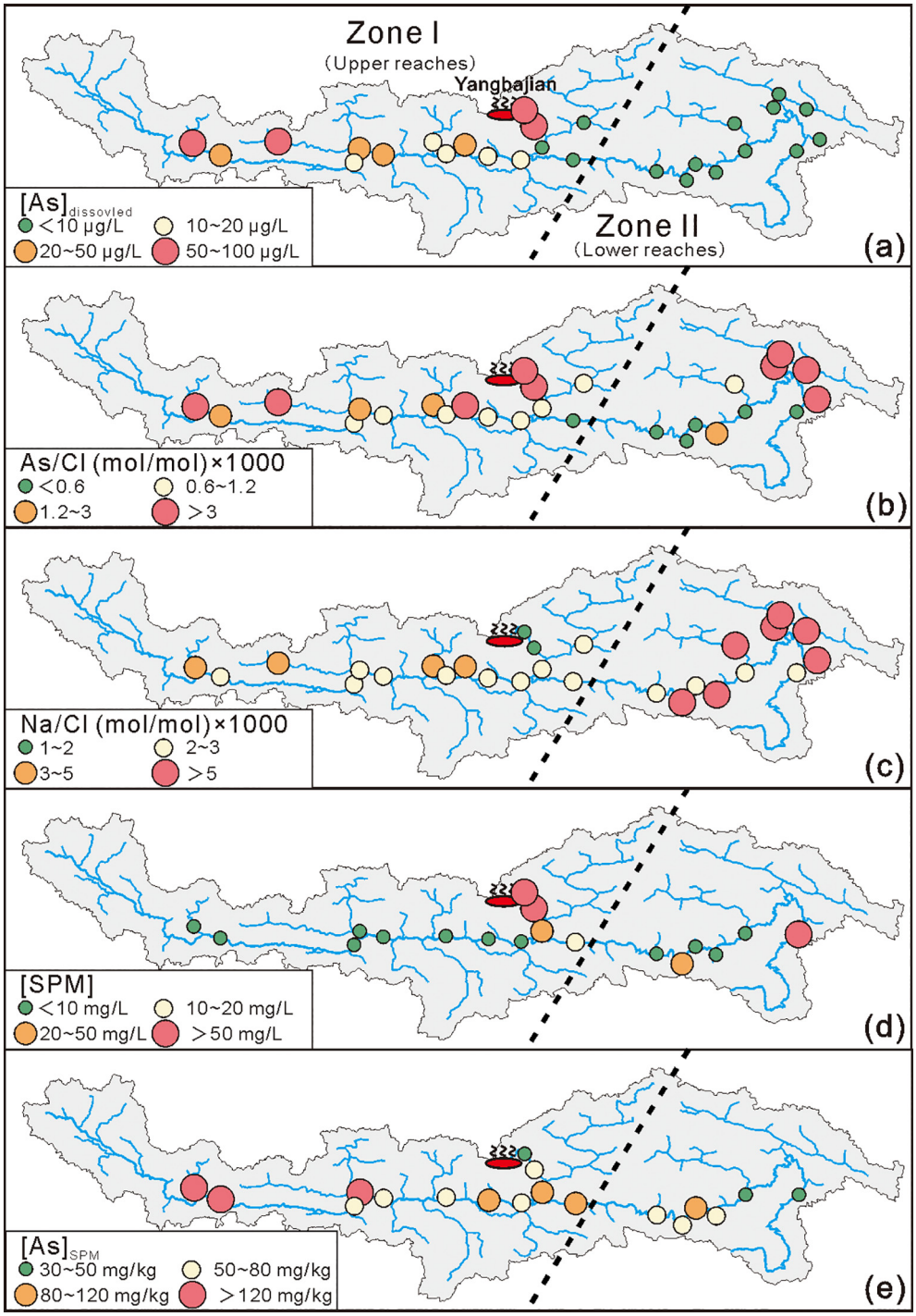

Fig. 3. Distribution of $[As]_{dissolved}$, $[As]_{SPM}$, SPM concentration, and As/Cl and Na/Cl ratios in YTR system.

removed from water (Fig. 7). Since the relatively few tributaries in the Dogxung Tsangbo, the variation in $[As]_{dissolved}$ and As/Na ratio in river water mainly reflect the geochemical process of the river itself. Thus, it can be speculated that adsorption and/or co-precipitation of As with metal oxides (or hydroxides) and/or other minerals (e.g., clays) may be the main reasons for the rapid removal of As from the tributaries. Usually, hot springs in TP have a strong reducing environment with reduced iron, manganese (e.g., Fe^{2+} and Mn^{2+}) and arsenite, as confirmed by the negatively Eh values and the relatively high concentrations of sulfide (Liu et al., 2018; Guo et al., 2019). After a hot spring is exposed to and mixed with stream water, the Fe^{2+} and Mn^{2+} will be immediately oxidized along with formation of oxides or hydroxides due to high levels of DO and weakly alkaline environments (Table 1). In addition, the arsenite is rapidly oxidized to arsenate, which is the dominant As species in the oxidizing environment and tends to be adsorbed by Fe and Mn oxides (or hydroxides) (Langner et al., 2001; Campbell and Nordstrom, 2014). Recent studies reported that the As is strongly adsorbed to primarily secondary Fe minerals (e.g., ferrihydrite, goethite, and hematite) and Mn oxides in river sediments (contaminated by hot springs) of TP (Zhang et al., 2017; Zhao et al., 2020). On the other hand, travertines, such as calcite and dolomite, formed near the outlet of hot spring can also remove some As by co-precipitation. Although the compositions of these samples are not analyzed in this study, previous studies in TP have confirmed that the travertine formed near hot springs is very

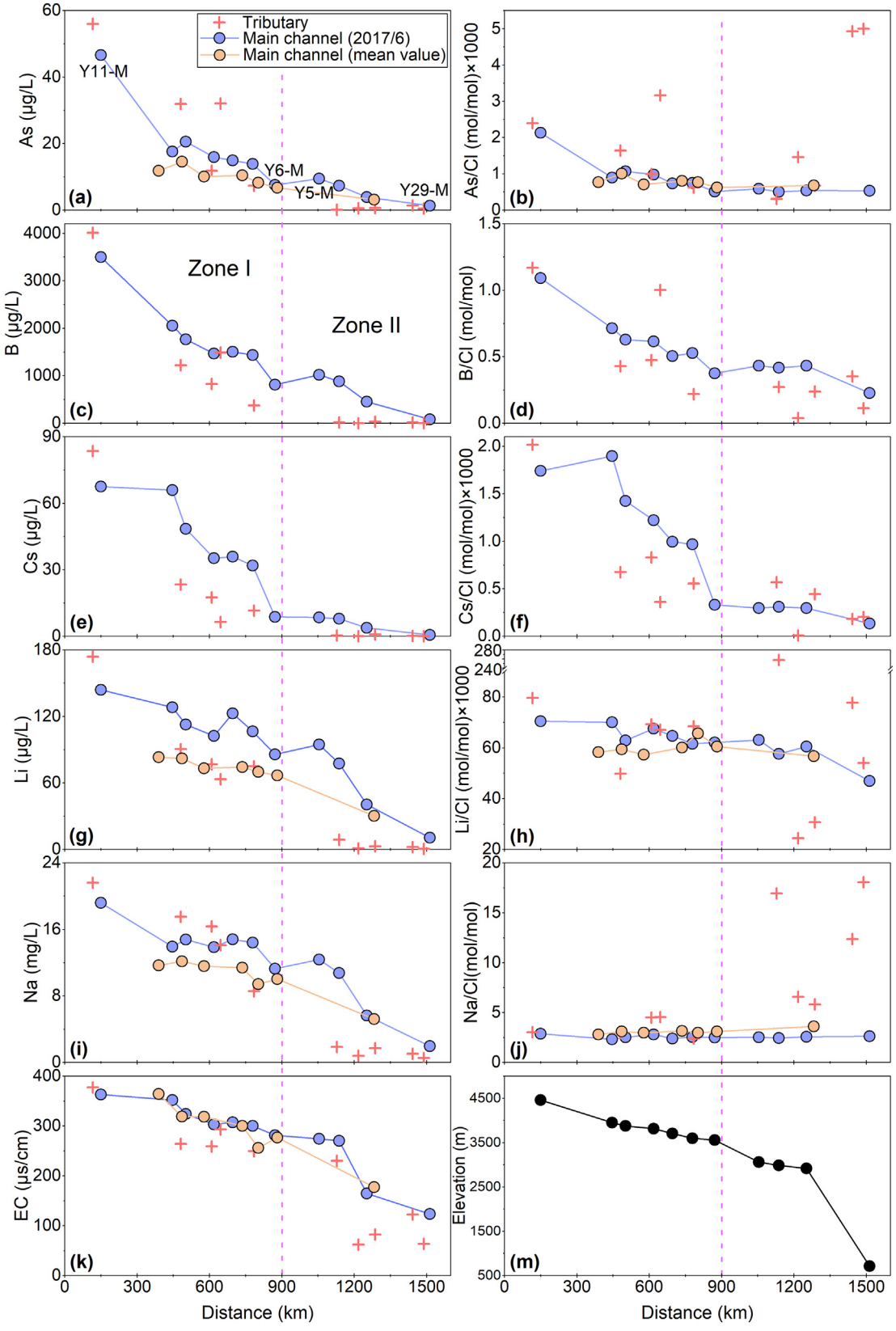

Fig. 4. Variations of chemical components and elevation along the river flow distance of YTR. The "+" and the circles represent tributary and main channel, respectively. The blue and orange circles represent the values (or mean values) of main channel samples collected in June 2017 and 2018, respectively. (For interpretation of the references to color in this figure legend, the reader is referred to the web version of this article.)

enriched in As (Feng et al., 2014). River sediments and SPM are good candidates for the adsorption of As. Previous studies in this area have also shown that sediments in tributaries polluted by hot springs are enriched in As, indicating that some of dissolved As in river water is removed by sediments (Guo et al., 2015). Likewise, in the present study, the SPM samples are enriched with As. However, similar to the main

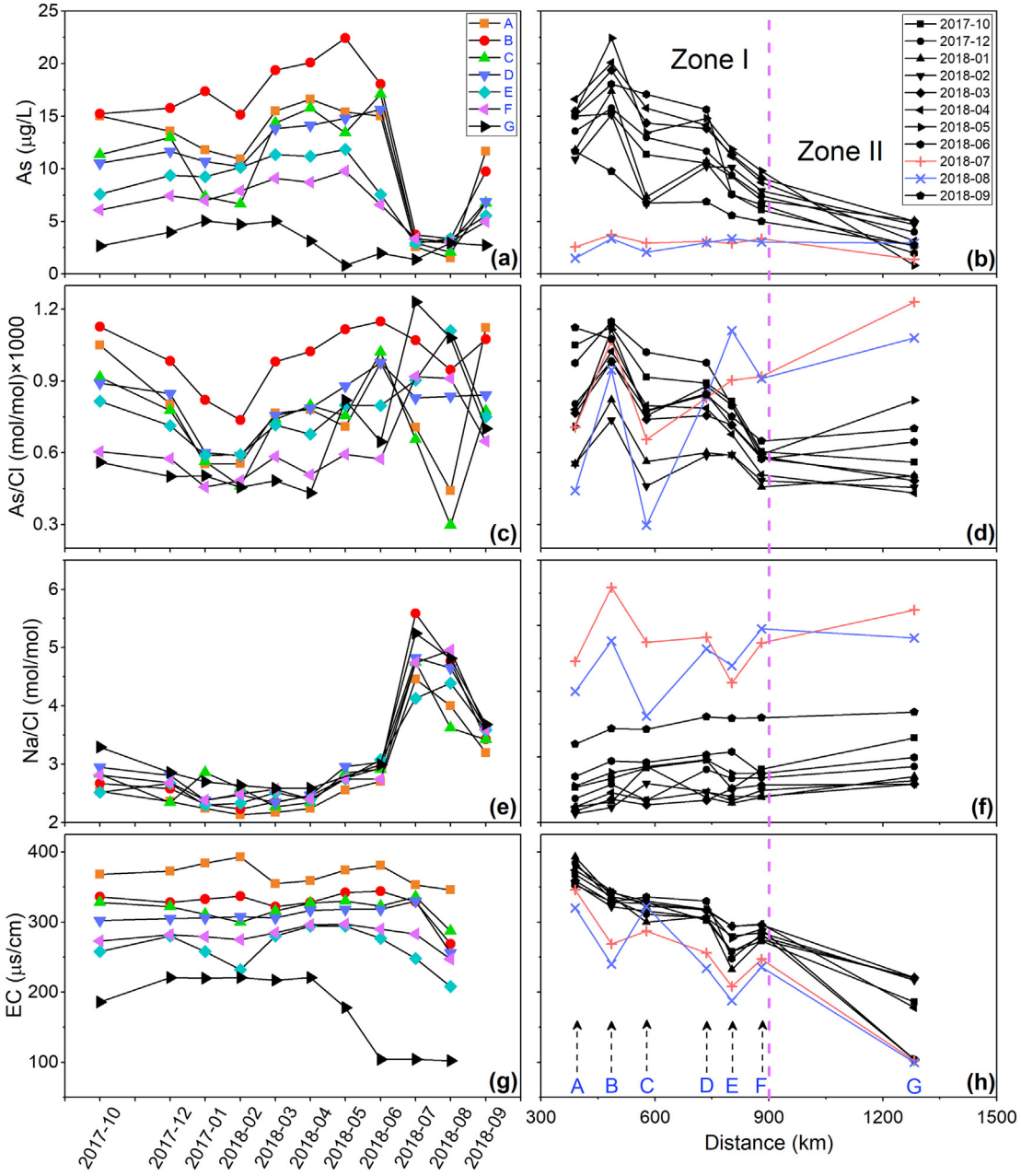

Fig. 5. Seasonal and spatial variations of chemical components ([As]dissolved, As/Cl, and Na/Cl) and EC values in the seven fixed sampling sites (site A to site G) from the main channel of YTR system. The locations of these fixed sampling sites are present in Fig. 1. The EC value of the sample in September 2018 was not measured.

channel, low concentration of SPM in most of the tributaries contributes little to the loss of As in the tributary water.

Another interesting observation is that the main channel data points of As vs. Cl (B vs. Cl and Cs vs. Cl) show two different trends in Zone I and Zone II (Fig. 6). Moreover, similar trends are observed in tributaries. This result may reflect that the different sources of As characterized by variations of $[As]_{dissolved}$ and As/Cl ratio from the tributaries. In Zone I, dissolved As in main channel directly sources from the influx of tributaries with high As concentration. Therefore, the trend 1 mainly reflects the variation in As/Cl ratio in tributaries. In Zone II, the trend 2 reflects the dilution process due to its almost parallel to the theoretical dilution line, which is consistent with the above conclusion (see Section 5.2.1). In addition, the river water chemical composition of Y6-M is the result of the elements undergoing all geochemical processes in Zone I, such as adsorption and/or co-precipitation, dilution, and mixing. In contrast, the $[As]_{dissolved}$ (and As/Cl ratio) in Y6-M is the initial value (or end member value) of the main channel going downstream in Zone II. Thus, due to the process of dilution, the As vs. Cl (B vs. Cl and Cs vs. Cl) data points of the main channel in Zone II fall on the new dilution line which is based on these data in Y6-M as the end member and parallel to the theoretical dilution line of hot springs. On the other hand, the $[As]_{dissolved}$, $[B]_{dissolved}$, and $[Li]_{dissolved}$ (As/Cl, B/Cl, and Li/Cl) in main channel slightly increased from sample Y6-M and Y5-M, suggesting that more these elements added to the main channel may from the un-sampled tributaries (or hot springs). Therefore, the variation characteristics of the element concentration and ratio in main channel may partially inherit that variation in tributary and hot spring (discussed in Section 5.4).

5.3. Seasonal variations of dissolved As in main channel river waters

The $[As]_{dissolved}$ in main channel river waters varies greatly with the seasons (1.4–22.4 μg/L), and is characterized by the lowest values (1.4–3.7 μg/L) in July and August (wet season), with the exception of

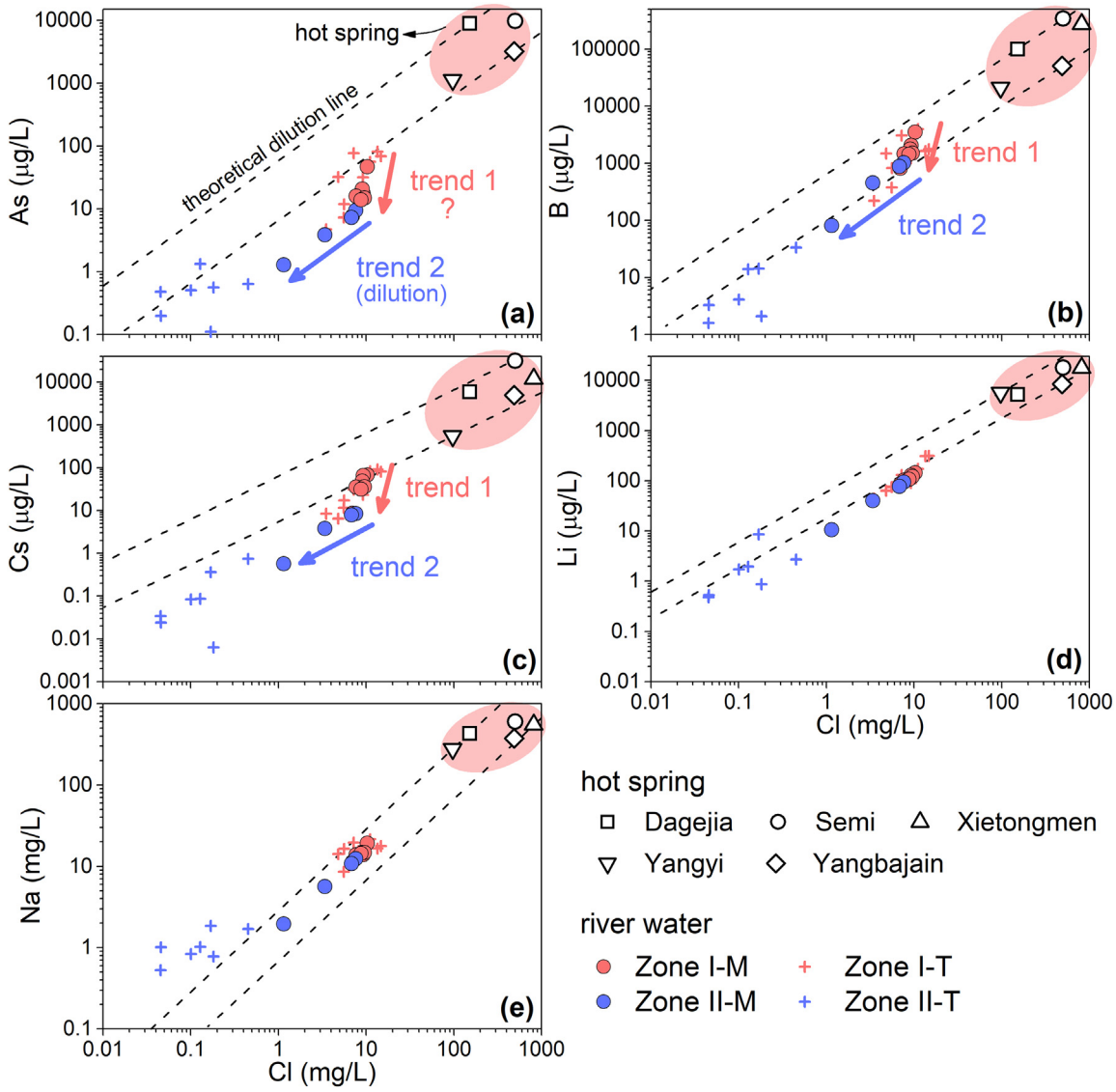

Fig. 6. The relationship between Na and Cl, X (X refers to As, B, Cs, Li) and Cl concentrations in river water and hot spring from YTR basin. The "-M" means the main channel and the "-T" means the tributary. The theoretical dilution lines are based on the assumption that the element concentrations of hot spring input river are only affected by dilution process.

the site G (Fig. 5(a)). The processes of dilution and adsorption (or co-precipitation) may decrease the As concentration in river water (Nimick et al., 1998; Guo et al., 2015). In the present study, the dilution is considered the main cause of the lowest $[As]_{dissolved}$ in river water in the two months. Main evidence is that the main channel discharge significantly increases in the wet season mainly due to increase of atmospheric precipitation and flux of melt waters from high mountains in this period (Fig. 2). Thus, these waters with low As concentrations recharge and dilute the river waters. The effect of dilution is also supported by the decrease in EC values in river waters in the two months (Fig. 5(g)). It is worth noting that the lowest $[As]_{dissolved}$ in river water collected in the site G is observed in May, because the site G is located the lower reaches with low altitude and entered the wet-season slightly earlier than the upper reaches. Removal of dissolved As through adsorption and/or co-precipitation process will reduce the As/Cl ratios in river water. However, most of river water As/Cl ratios increase in the two months. Therefore, the effect of adsorption and/or co-precipitation of dissolved As on the decrease in $[As]_{dissolved}$ in river waters is not significant in the wet season.

Weathering of As-containing rocks and minerals may have an important contribution to the $[As]_{dissolved}$ in YTR waters in the wet-season. Most of As/Cl ratios showed an increasing tendency from February to August, suggesting more As was added to the river water in this period. Since the hot springs have relatively stable As/Cl ratios, there should be other sources of As released into the river water. Arsenic is relatively enriched in Fe-S minerals (e.g., FeS, FeS_2 and FeAsS) and As-S minerals (e.g., As_4S_4 and As_2S_3). Thus, it can be speculated that weathering of sulfide minerals is an important source of As in river water (Saunders et al., 2005). In the wet season, increased atmospheric precipitation (containing O_2 and H_2O) will accelerate the oxidation of sulfide minerals (Eqs. (1) to (3)). This speculation is consistent with previous study results in the upper reaches of Yellow River that the oxidation of sulfide minerals increases in the wet-season in TP (Zhang et al., 2020). From our recent study, enhanced oxidation of sulfide minerals in the wet-season has been confirmed by sulfur isotopes in river water of YTR basin (unpublished data). On the other hand, in July and August, the increasing trend of As/Cl ratios from site A to site G also supports this speculation (Fig. 5(b)). Assuming that the hot spring is the only source of As in river water in the two months, the $[As]_{dissolved}$ in main channel will be decreased from site A to site G due to the dilution process, such as the variations of $[As]_{dissolved}$ in river water from the rest of months. However, the $[As]_{dissolved}$ is relatively stable in river water in

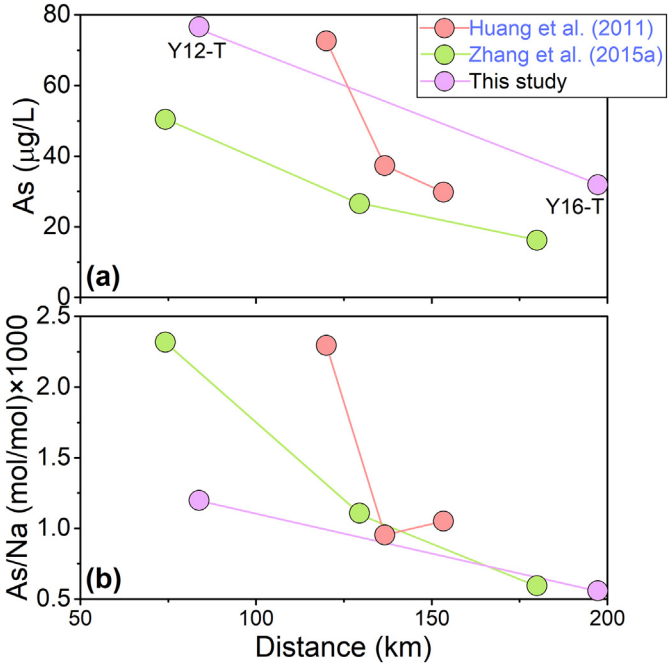

Fig. 7. Variations of $[As]_{dissolved}$ and As/Na ratio along the river flow distance of the Dogxung Tsangbo.

the two months. Therefore, significant $[As]_{dissolved}$ from other sources (e.g., oxidation of sulfide minerals) may be added into river water in the wet season, which offsets the effect of dilution process.

$$FeS_2 + O_2 + H_2O \rightarrow Fe(OH)_3 + SO_4^{2-} + H^+ \quad (1)$$

$$FeAsS + O_2 + H_2O \rightarrow Fe(OH)_3 + SO_4^{2-} + H_3AsO_3/HAsO_4^{2-} + H^+ \quad (2)$$

$$As_2S_3 + O_2 + H_2O \rightarrow SO_4^{2-} + H_3AsO_3/HAsO_4^{2-} + H^+ \quad (3)$$

5.4. Ratio of As/Cl decreases in tributaries distributed from upper to lower reaches

It is worth noting that the As/Cl (B/Cl and Cs/Cl) ratio decreases in tributaries distributed from the upper to lower reaches (east to west) of YTR basin (Fig. 4). Similar results are observed in hot springs, tributaries, and main channel water samples collected from the east to west of the basin (Fig. 8). There are few reports of similar observations in this area, while previous studies suggested that the variation in B/Cl ratio (or $[B]_{dissolved}$) in hot springs of TP may reflect the different sources of B, such as magmatic sources and host rocks (Lü et al., 2014; W. Zhang et al., 2015). The As/Cl ratio (or $[As]_{dissolved}$) in hot springs may have temporal or spatial variability. However, the dissolved As concentration of the hot spring sample is very close to the values that reported from previous studies at the same geothermal field (e.g., the Yangbajin) (see details in Section 4.1), suggesting the effect of temporal variability on As concentration of the hot spring is not significant. From Fig. 8(a), the As/Cl ratio (or As/Na) in hot springs has significant spatial variability and show a decrease trend from west to east of YTR basin. Accordingly, since the As (B and Cs) in tributaries mainly sources from hot springs in YTR basin, the trend of As/Cl ratio in tributaries can be explained in two ways. First, the hot springs have different sources of As with varying As/Cl ratio. Second, the As/Cl ratio in hot springs changed significantly during the water-rock interactions accompanying the groundwater flow.

We hypothesize that groundwater flow path and residence time could be significant factors resulting in the decrease in As/Cl (B/Cl and Cs/Cl) ratio in hot springs distributed from the east to west of YTR basin, which in turn partly causes these ratios decrease in tributaries and main channel. Drawing the groundwater flow system is helpful to analyze the link between river water and groundwater in this basin. Unfortunately, the limited groundwater data in this study cannot accurately delineate the groundwater flow system in the basin. However, according to previous studies, there could be three major groundwater flow paths in YTR basin: groundwater flow from two margin areas towards the middle of the basin; and that from west to east along the Indus-Tsangpo suture (Fig. S5). The characteristics of hydrogen and oxygen isotopes data of geothermal water, river, and lakes water suggested that local atmospheric precipitation (including rainfall, snow, and glacial melt water) is the main recharge source of geothermal water in TP (Tan et al., 2014). Groundwater is recharged by precipitation at high altitudes and vertically infiltrated and deeply circulated (up to ~2 km in depth) along geological fault-fractures or fissures, and is discharged eventually as springs in basins and valleys (Ge et al., 2008; Cheng and Jin, 2013). Thus, groundwater flow in TP is usually driven and sustained topographically (recharged at high elevations and discharged at low areas) (Ge et al., 2008). Overall, the topography of YTR basin is characterized by high elevations to the west and low elevations to the east. The southern and northern boundaries of the basin are the Himalayas and Gangdese Mountains, respectively (see Section 2). The middle of the basin has the lowest elevations and YTR flows eastward on the plain along the Indus-Tsangpo suture.

Groundwater with different flow paths and residence times in TP influence not only hydrological cycle but also chemical compositions of groundwater and surface water (Tipper et al., 2006; Andermann et al., 2012; Z. Yu et al., 2019). Generally, groundwater residence time (or water-rock interaction time) increases with an increase in the groundwater flow path (Edmunds and Smedley, 2000). Thus, the active elements (e.g., B, Cs, and Mg) will be partly removed by newly-formed secondary minerals (e.g., clays, metal oxy-hydroxides, and carbonate) from groundwater though adsorption and/or co-precipitation along the groundwater flow path (Edmunds et al., 2003; Zhang et al., 2018). As a result, the ratio of the active element (As, B, and Cs) to inert (or non-conservative) element Na or Cl in groundwater gradually decreases with an increase in groundwater flow path, and further significant decreases in these ratios in tributary and main channel in lower reaches of the basin (Fig. S5).

6. Conclusion

Enrichment of dissolved As (B, Cs, and Li) is observed in river waters in upper reaches (Zone I) of the Yarlung Tsangpo River (YTR) as well as extremely high As concentration (mg/L) in hot springs, while low levels of As are largely found in tributaries of lower reaches (Zone II). In addition, the $[As]_{dissolved}$ varies greatly with seasons in main channel during the sampling time period, and the low $[As]_{dissolved}$ is largely observed in July and August 2018 (wet-season). Hot springs could be the main source for the elevated As (B, Cs and Li) in YTR. Although the river water in the upper reaches are enriched with As, $[As]_{dissolved}$ in main channel is reduced by several ten-fold in the low reaches. Natural attenuation of As in main channel is dominated by dilution process, but mostly occurred by both dilution and adsorption (or co-precipitation) processes in tributaries. Results from seasonal variations of $[As]_{dissolved}$ in main channel suggest that weathering of As-containing rocks and minerals may have an important contribution to the $[As]_{dissolved}$ in YTR waters in the wet-season. The geochemical behavior of As is largely transported conservatively in the main channel and relative non-conservatively in the tributaries in YTR system. Groundwater flow path and residence time could be significant factors resulting in the decrease in As/Cl (B/Cl and Cs/Cl) ratio in hot springs distributed from the east to west of YTR basin, which in turn partly causes these ratios decrease in tributaries and main channel in lower reaches. Nonetheless, future studies are needed to further refine the groundwater flow system

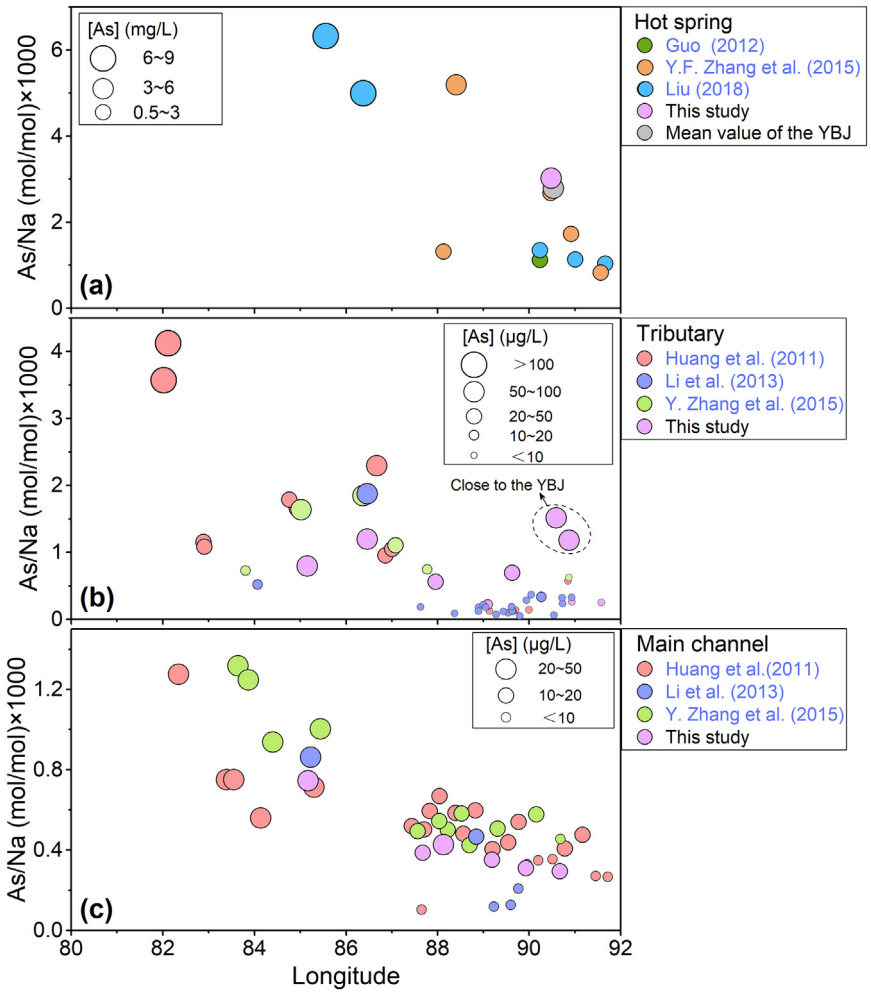

Fig. 8. Variations of As/Na ratio in hot spring, tributary and main channel distributed from upper to lower reaches of YTR basin. Since there is no [Cl]dissolved data in some references, we use As/Na ratio instead of As/Cl ratio. Our data shows that the Na/Cl is relatively constant throughout the year, except for July, August and September (Fig. 5). The sampling time of these references is not in the three months. Therefore, the trend of As/Na ratio here should be similar to that of As/Cl ratio in hot spring, tributary and main channel distributed from upper to lower reaches of YTR basin.

in the study area in order to evaluate the link between river water and groundwater in YTR basin.

CRediT authorship contribution statement

Jun-Wen Zhang: Data curation, Formal analysis, Investigation, Methodology, Resources, Writing - original draft, Writing - review & editing. **Ya-Ni Yan:** Formal analysis, Methodology, Resources, Writing - original draft, Writing - review & editing. **Zhi-Qi Zhao:** Conceptualization, Formal analysis, Funding acquisition, Investigation, Project administration, Resources, Supervision, Validation, Writing - original draft, Writing - review & editing. **Xiao-Dong Li:** Formal analysis, Supervision, Validation, Writing - original draft, Writing - review & editing. **Jian-Yang Guo:** Formal analysis, Funding acquisition, Investigation, Writing - review & editing. **Hu Ding:** Investigation, Resources, Writing - review & editing. **Li-Feng Cui:** Investigation, Resources. **Jun-Lun Meng:** Investigation, Resources. **Cong-Qiang Liu:** Conceptualization, Project administration, Supervision, Validation, Writing - review & editing.

Declaration of competing interest

The authors declare that they have no known competing financial interests or personal relationships that could have appeared to influence the work reported in this paper.

Acknowledgements

The authors would like to thank the four anonymous reviews for their constructive suggestions and comments on this manuscript. We thank Gao Shuang, Jia Guodong, Zhang Xiaolong, Yang Ye, Liu Xu, and Ye Runcheng for helping the field work. This work was supported jointly by the National Natural Science Foundation of China (No. 41930863, 91647205, 41661144042), and the Second Tibetan Plateau Scientific Expedition and Research (2019QZKK0707), and Special Fund for Basic Scientific Research of Central Colleges, Chang'an University (No. 3001102278302).

Appendix A. Supplementary data

Supplementary data to this article can be found online at https://doi.org/10.1016/j.scitotenv.2020.143416.

References

Aitchison, J.C., Davis, A.M., Luo, H., 2002. New constraints on the India–Asia collision: the lower Miocene Gangrinboche conglomerates, Yarlung Tsangpo suture zone, SE Tibet. J. Asian Earth Sci. 21 (3), 251–263.

Andermann, C., Longuevergne, L., Bonnet, S., Crave, A., Davy, P., Gloaguen, R., 2012. Impact of transient groundwater storage on the discharge of Himalayan rivers. Nat. Geosci. 5 (2), 127.

Ball, J.W., McMleskey, R.B., Nordstrom, D.K., 2010. Water-Chemistry Data for Selected Springs, Geysers, and Streams in Yellowstone National Park, Wyoming, 2006–2008 (No. 2010-1192). US Geological Survey.

Campbell, K.M., Nordstrom, D.K., 2014. Arsenic speciation and sorption in natural environments. Rev. Mineral. Geochem. 79 (1), 185–216.

Cheng, G., Jin, H., 2013. Permafrost and groundwater on the Qinghai-Tibet Plateau and in northeast China. Hydrogeol. J. 21 (1), 5–23.

Concha, G., Broberg, K., Grandér, M., Cardozo, A., Palm, B., Vahter, M., 2010. High-level exposure to lithium, boron, cesium, and arsenic via drinking water in the Andes of northern Argentina. Environ. Sci. Technol. 44 (17), 6875–6880.

Edmunds, W.M., Smedley, P.L., 2000. Residence time indicators in groundwater: the East Midlands Triassic sandstone aquifer. Appl. Geochem. 15 (6), 737–752.

Edmunds, W.M., Guendouz, A.H., Mamou, A., Moulla, A., Shand, P., Zouari, K., 2003. Groundwater evolution in the Continental Intercalaire aquifer of southern Algeria and Tunisia: trace element and isotopic indicators. Appl. Geochem. 18 (6), 805–822.

Fendorf, S., Michael, H.A., Geen, A.V., 2010. Spatial and temporal variations of groundwater arsenic in South and Southeast Asia. Science 328 (5982), 1123–1127.

Feng, J.L., Zhao, Z.H., Chen, F., Hu, H.P., 2014. Rare earth elements in sinters from the geothermal waters (hot springs) on the Tibetan Plateau, China. J. Volcanol. Geotherm. Res. 287, 1–11.

Gaillardet, J., Viers, J., Dupré, B., 2003. Trace elements in river waters. Treatise Geochem. 5, 605.

Gao, Z., Wang, X., Yin, G., 2007. Hydrological rule and isotopic composition of water bodies in Yarlung Zangbo River. Acta Geograph. Sin. 62 (9), 1002–1007 (in Chinese with English abstract).

Ge, S., Wu, Q.B., Lu, N., Jiang, G.L., Ball, L., 2008. Groundwater in the Tibet Plateau, western China. Geophys. Res. Lett. 35 (18).

Guillot, S., Charlet, L., 2007. Bengal arsenic, an archive of Himalaya orogeny and paleohydrology. J. Environ. Sci. Health A 42 (12), 1785–1794.

Guo, Q., 2012. Hydrogeochemistry of high-temperature geothermal systems in China: a review. Appl. Geochem. 27 (10), 1887–1898.

Guo, Q., Wang, Y., Liu, W., 2008. B, As, and F contamination of river water due to wastewater discharge of the Yangbajing geothermal power plant, Tibet, China. Environ. Geol. 56 (1), 197–205.

Guo, Q., Cao, Y., Li, J., Zhang, X., Wang, Y., 2015. Natural attenuation of geothermal arsenic from Yangbajain power plant discharge in the Zangbo River, Tibet, China. Appl. Geochem. 62, 164–170.

Guo, Q., Planer-Friedrich, B., Liu, M., Yan, K., Wu, G., 2019. Magmatic fluid input explaining the geochemical anomaly of very high arsenic in some southern Tibetan geothermal waters. Chem. Geol. 513, 32–43.

Hren, M.T., Chamberlain, C.P., Hilley, G.E., Blisniuk, P.M., Bookhagen, B., 2007. Major ion chemistry of the Yarlung Tsangpo–Brahmaputra river: chemical weathering, erosion, and CO_2 consumption in the southern Tibetan plateau and eastern syntaxis of the Himalaya. Geochim. Cosmochim. Acta 71 (12), 2907–2935.

Hu, Z., Gao, S., 2008. Upper crustal abundances of trace elements: a revision and update. Chem. Geol. 253 (3–4), 205–221.

Huang, X., Sillanpää, M., Duo, B.U., Gjessing, E.T., 2008. Water quality in the Tibetan plateau: metal contents of four selected rivers. Environ. Pollut. 156 (2), 270–277.

Huang, X., Sillanpää, M., Gjessing, E.T., Peräniemi, S., Vogt, R.D., 2011. Water quality in the southern Tibetan Plateau: chemical evaluation of the Yarlung Tsangpo (Brahmaputra). River Res. Appl. 27 (1), 113–121.

Islam, S.M.N., Rahman, S.H., Chowdhury, D.A., Rahman, M.M., Tareq, S.M., 2012. Seasonal variations of arsenic in the Ganges and Brahmaputra River, Bangladesh. J. Sci. Res. 4 (1), 65–75.

Kearey, P., Wei, H., 1993. Geothermal fields of China. J. Volcanol. Geotherm. Res. 56 (4), 415–428.

Langner, H.W., Jackson, C.R., Mcdermott, T.R., Inskeep, W.P., 2001. Rapid oxidation of arsenite in a hot spring ecosystem, Yellowstone National Park. Environ. Sci. Technol. 35 (16), 3302–3309.

Li, Z.Q., 2002. Present Hydrothermal Activities during Collisional Orogenics of the Tibetan Plateau. Doctoral dissertation, Ph. D. Thesis. Chinese Academy of Geological Sciences, Beijing, China (In Chinese with English Abstract).

Li, S., Wang, M., Yang, Q., Wang, H., Zhu, J., Zheng, B., Zheng, Y., 2013. Enrichment of arsenic in surface water, stream sediments and soils in Tibet. J. Geochem. Explor. 135, 104–116.

Li, C., Kang, S., Chen, P., Zhang, Q., Mi, J., Gao, S., Sillanpää, M., 2014a. Geothermal spring causes arsenic contamination in river waters of the southern Tibetan Plateau, China. Environ. Earth Sci. 71 (9), 4143–4148.

Li, F., Xu, Z., Liu, W., Zhang, Y., 2014b. The impact of climate change on runoff in the Yarlung Tsangpo River basin in the Tibetan Plateau. Stoch. Env. Res. Risk A. 28 (3), 517–526.

Liu, T., 1999. Hydrological characteristics of Yalungzangbo River. Acta Geograph. Sin. 54 (Suppl), 157–164 (in Chinese, with English abstract).

Liu, M., 2018. Boron Geochemistry of the Geothermal Waters From Typical Hydrothermal Systems in Tibet. Doctoral dissertation, Ph. D. Thesis. China University of Geoscience (In Chinese with English Abstract).

Liu, J., Yao, Z., Chen, C., 2007. Evolution trend and causation analysis of the runoff evolution in the Yarlung Zangbo river basin. J. Nat. Resour. 22 (3), 471–477 (in Chinese with English Abstract).

Liu, M., Guo, Q., Wu, G., Guo, W., She, W., Yan, W., 2019. Boron geochemistry of the geothermal waters from two typical hydrothermal systems in Southern Tibet (China): Daggyai and Quzhuomu. Geothermics 82, 190–202.

Lü, Y., Zheng, M., Zhao, P., Xu, R., 2014. Geochemical processes and origin of boron isotopes in geothermal water in the Yunnan-Tibet geothermal zone. Sci. China Earth Sci. 57 (12), 2934–2944.

Masson, M., Schäfer, J., Blanc, G., Pierre, A., 2007. Seasonal variations and annual fluxes of arsenic in the Garonne, Dordogne and Isle Rivers, France. Sci. Total Environ. 373 (1), 196–207.

Mukherjee, A. (Ed.), 2018. Groundwater of South Asia. Springer.

Mukherjee, A., Verma, S., Gupta, S., Henke, K.R., Bhattacharya, P., 2014. Influence of tectonics, sedimentation and aqueous flow cycles on the origin of global groundwater arsenic: paradigms from three continents. J. Hydrol. 518, 284–299.

Muñoz, M.O., Bhattacharya, P., Sracek, O., Ramos, O.R., Aguirre, J.Q., Bundschuh, J., Maity, J.P., 2015. Arsenic and other trace elements in thermal springs and in cold waters from drinking water wells on the Bolivian Altiplano. J. S. Am. Earth Sci. 60, 10–20.

Nickson, R., McArthur, J., Burgess, W., Ahmed, K.M., Ravenscroft, P., Rahmanñ, M., 1998. Arsenic poisoning of Bangladesh groundwater. Nature 395 (6700), 338.

Nickson, R.T., McArthur, J.M., Ravenscroft, P., Burgess, W.G., Ahmed, K.M., 2000. Mechanism of arsenic release to groundwater, Bangladesh and West Bengal. Appl. Geochem. 15 (4), 403–413.

Nimick, D.A., Moore, J.N., Dalby, C.E., Savka, M.W., 1998. The fate of geothermal arsenic in the Madison and Missouri Rivers, Montana and Wyoming. Water Resour. Res. 34 (11), 3051–3067.

Nordstrom, D.K., 2002. Worldwide occurrences of arsenic in ground water. Science 296, 2143–2145.

Nordstrom, D.K., 2009. Natural arsenic enrichment: effects of diagenetic-tectonichydrothermal cycle. Geol. Soc. Am. Abstr. Program 41 (7), 217.

Nordstrom, D.K., Ball, J.W., McCleskey, R.B., 2005. Ground water to surface water: chemistry of thermal outflows in Yellowstone National Park. Geothermal Biology and Geochemistry in Yellowstone National Park, pp. 73–94.

Qu, B., Zhang, Y., Kang, S., Sillanpää, M., 2019. Water quality in the Tibetan Plateau: major ions and trace elements in rivers of the "Water Tower of Asia". Sci. Total Environ. 649, 571–581.

Romero, L., Alonso, H., Campano, P., Fanfani, L., Cidu, R., Dadea, C., Keegan, T., Thornton, I., Farago, M., 2003. Arsenic enrichment in waters and sediments of the Rio Loa (Second Region, Chile). Appl. Geochem. 18 (9), 1399–1416.

Roy, S., Gaillardet, J., Allegre, C.J., 1999. Geochemistry of dissolved and suspended loads of the Seine river, France: anthropogenic impact, carbonate and silicate weathering. Geochim. Cosmochim. Acta 63 (9), 1277–1292.

Saunders, J.A., Lee, M.K., Uddin, A., Mohammad, S., Wilkin, R.T., Fayek, M., Korte, N.E., 2005. Natural arsenic contamination of Holocene alluvial aquifers by linked tectonic, weathering, and microbial processes. Geochem. Geophys. Geosyst. 6 (4).

Sharifi, R., Moore, F., Keshavarzi, B., 2016. Mobility and chemical fate of arsenic and antimony in water and sediments of Sarouq River catchment, Takab geothermal field, northwest Iran. J. Environ. Manag. 170, 136–144.

Smedley, P.L., Kinniburgh, D.G., 2002. A review of the source, behaviour and distribution of arsenic in natural waters. Appl. Geochem. 17, 517–568.

Smedley, P.L., Kinniburgh, D.G., 2013. Arsenic in groundwater and the environment. Essentials of Medical Geology. Springer, Netherlands, pp. 279–310.

Tan, H., Zhang, Y., Zhang, W., Kong, N., Zhang, Q., Huang, J., 2014. Understanding the circulation of geothermal waters in the Tibetan Plateau using oxygen and hydrogen stable isotopes. Appl. Geochem. 51, 23–32.

Tapia, J., Murray, J., Ormachea, M., Tirado, N., Nordstrom, D.K., 2019. Origin, distribution, and geochemistry of arsenic in the Altiplano-Puna plateau of Argentina, Bolivia, Chile, and Perú. Sci. Total Environ. 678, 309–325.

Tian, Y., Yu, C., Zha, X., Wu, J., Gao, X., Feng, C., Luo, K., 2016. Distribution and potential health risks of arsenic, selenium, and fluorine in natural waters in Tibet, China. Water 8 (12), 568.

Tipper, E.T., Bickle, M.J., Galy, A., West, A.J., Pomiès, C., Chapman, H.J., 2006. The short term climatic sensitivity of carbonate and silicate weathering fluxes: insight from seasonal variations in river chemistry. Geochim. Cosmochim. Acta 70 (11), 2737–2754.

Wang, M., Li, S., Wang, H., Xiao, T., Zheng, B., 2012. Distribution of arsenic in surface water in Tibet. Environ. Sci. 33 (10), 3411–3416 (In Chinese with English Abstract).

Wang, Y., Pi, K., Fendorf, S., Deng, Y., Xie, X., 2017. Sedimentogenesis and hydrobiogeochemistry of high arsenic Late Pleistocene-Holocene aquifer systems. Earth Sci. Rev. 189, 79–98.

WHO, 2011. Guideline for Drinking-water Quality. 4th ed. World Health Organization, Geneva, Switzerland, p. 564.

Xu, X., Lu, C., Shi, X., Gao, S., 2008. World water tower: an atmospheric perspective. Geophys. Res. Lett. 35 (20).

You, Q., Kang, S., Wu, Y., Yan, Y., 2007. Climate change over the Yarlung Zangbo river basin during 1961–2005. J. Geogr. Sci. 17 (4), 409–420.

Yu, J., Gao, C., Cheng, A., Liu, Y., Zhang, L., He, X., 2013. Geomorphic, hydroclimatic and hydrothermal controls on the formation of lithium brine deposits in the Qaidam Basin, northern Tibetan Plateau, China. Ore Geol. Rev. 50, 171–183.

Yu, C., Sun, Y., Zhong, X., Yu, Z., Li, X., Yi, P., Jin, H., Luo, D., 2019a. Arsenic in permafrost-affected rivers and lakes of Tibetan Plateau, China. Environ. Pollutants Bioavailab. 31 (1), 226–232.

Yu, Z., Wu, G., Keys, L., Li, F., Yan, N., Qu, D., Liu, X., 2019b. Seasonal variation of chemical weathering and its controlling factors in two alpine catchments, Nam Co basin, central Tibetan Plateau. J. Hydrol. 576, 381–395.

Yuan, J., Guo, Q., Wang, Y., 2014. Geochemical behaviors of boron and its isotopes in aqueous environment of the Yangbajing and Yangyi geothermal fields, Tibet, China. J. Geochem. Explor. 140, 11–22.

Zhang, Y., Sillanpää, M., Li, C., Guo, J., Qu, B., Kang, S., 2015a. River water quality across the Himalayan regions: elemental concentrations in headwaters of Yarlung Tsangbo, Indus and Ganges River. Environ. Earth Sci. 73 (8), 4151–4163.

Zhang, Y.F., Tan, H.B., Zhang, W.J., Huang, J.Z., Zhang, Q., 2015b. A new geochemical perspective on hydrochemical evolution of the Tibetan geothermal system. Geochem. Int. 53 (12), 1090–1106.

Zhang, W., Tan, H., Zhang, Y., Wei, H., Dong, T., 2015c. Boron geochemistry from some typical Tibetan hydrothermal systems: origin and isotopic fractionation. Appl. Geochem. 63, 436–445.

Zhang, Y., Li, S., Zheng, L., Chen, J., Zheng, Y., 2017. Evaluation of arsenic sorption and mobility in stream sediment and hot spring deposit in three drainages of the Tibetan Plateau. Appl. Geochem. 77, 89–101.

Zhang, H., Jiang, X.W., Wan, L., Ke, S., Liu, S.A., Han, G., Guo, H.M., Dong, A., 2018. Fractionation of Mg isotopes by clay formation and calcite precipitation in groundwater with long residence times in a sandstone aquifer, Ordos Basin, China. Geochim. Cosmochim. Acta 237, 261–274.

Zhang, D., Zhao, Z.Q., Li, X.D., Zhang, L.L., Chen, A.C., 2020. Assessing the oxidative weathering of pyrite and its role in controlling atmospheric CO_2 release in the eastern Qinghai-Tibet Plateau. Chem. Geol. 543, 119605.

Zhao, Z., Li, S., Xue, L., Liao, J., Zhao, J., Wu, M., Wang, M., Sun, J., Zheng, Y., Yang, Q., 2020. Effects of dam construction on arsenic mobility and transport in two large rivers in Tibet, China. Sci. Total Environ. 741, 140406.

Zheng, M., Liu, X., 2009. Hydrochemistry of salt lakes of the Qinghai-Tibet Plateau, China. Aquat. Geochem. 15 (1–2), 293–320.